Journal of Maps

ISSN: (Print) (Online) Journal homepage: https://www.tandfonline.com/loi/tjom20

Structural setting and architecture of the North Cycladic Detachment System in the northeastern sectors of Mykonos Island (Greece)

Raffaele Gazzola, Costantino Zuccari, Chiara Frassi, Paraskevas Xypolias & Giovanni Musumeci

To cite this article: Raffaele Gazzola, Costantino Zuccari, Chiara Frassi, Paraskevas Xypolias & Giovanni Musumeci (2023) Structural setting and architecture of the North Cycladic Detachment System in the northeastern sectors of Mykonos Island (Greece), Journal of Maps, 19:1, 2277387, DOI: 10.1080/17445647.2023.2277387

To link to this article: https://doi.org/10.1080/17445647.2023.2277387

JOURNAL OF MAPS
2023, VOL. 19, NO. 1, 2277387
https://doi.org/10.1080/17445647.2023.2277387

Structural setting and architecture of the North Cycladic Detachment System in the northeastern sectors of Mykonos Island (Greece)

Raffaele Gazzola[a], Costantino Zuccari[a], Chiara Frassi[a], Paraskevas Xypolias[b] and Giovanni Musumeci[a,b,c]

[a]Department of Earth Sciences, University of Pisa, Pisa, Italy; [b]Department of Geology, University of Patras, Patras, Greece; [c]Istituto Nazionale di Geofisica e Vulcanologia, Sezione Pisa, Pisa, Italy

ABSTRACT

We present the 1:8000 scale geological map of the northeastern sector of Mykonos Island, where an igneous, metamorphic and siliciclastic sequence is cut by the North Cycladic Detachment System (NCDS), and brittly-ductily deformed during the emplacement of the Mykonos Granite. We describe the architecture of the (ductile) Livada and (brittle) Mykonos Detachments pertaining to the NCDS. Geological mapping was functional to (i) the description of along and across strike geometrical variations of the detachments and (ii) the analysis of the deformation and strain partitioning within the deformed rocks. We show that deformation localisation differs along dip and strike for the Mykonos Detachment, which accommodated deformation both through thick and localised fault zones. Also, the ductile fabric of the Livada Detachment is characterised by a strong strain localisation, which generally decreases from eastwards. Moreover, the geological map shows that the detachments orientation allowed the local elision of the original tectono-stratigraphy.

ARTICLE HISTORY
Received 28 June 2023
Revised 17 October 2023
Accepted 23 October 2023

KEYWORDS
Mykonos Detachment; brittle-ductile deformation; North Cycladic Detachment System; Aegean rift; Cyclades

1. Introduction

The Aegean Region and especially the Cyclades represent an excellent natural laboratory to study the superposition of multiple tectonic phases, which occurred since the Africa-Europe plate convergence stage up to the post-orogenic slab-retreat and extension processes (eg Agostini et al., 2010; Brichau et al., 2006; Jolivet et al., 2013; Jolivet & Brun, 2010; Le Pichon & Angelier, 1981). The structural analysis and mapping of tectonic structures nowadays exposed in the Cyclades also allow the understanding of mechanisms and processes that govern the formation of Metamorphic Core Complexes (MCCs), a major crustal-scale structure which has been described in several areas worldwide (eg Lister et al., 1984; Lister & Baldwin, 1993; Platt et al., 2015; Searle & Lamont, 2020). It is broadly accepted that the present configuration of the Cyclades is related to the formation of a series of MCCs, which are genetically associated with the emplacement of large plutonic (granite) intrusions (eg Bakowsky et al., 2023; Cao et al., 2013; Faure et al., 1991; Grasemann et al., 2012; Lamont et al., 2023a; Pe-Piper et al., 2002). The emplacement of plutonic intrusions and the MCCs formation were accommodated at different crustal depths in the Cyclades by regional ductile shear zones and brittle detachments that allowed the progressive post-orogenic exhumation of units that underwent HP-LT syn-orogenic metamorphism (eg Grasemann et al., 2012; Jolivet & Brun, 2010; Jolivet & Faccenna, 2000; Lee & Lister, 1992; Mehl et al., 2005). These shear zones and detachments were grouped into the North Cycladic Detachment System (NCDS), the West Cycladic Detachment System (WCDS), the Naxos-Paros Detachment System (NPDS) and the South Cycladic Detachment System (SCDS) (eg Grasemann et al., 2018; Ring et al., 2011).

Among other islands and localities in the Aegean Sea (eg Tinos, Andros, Ikaria; Figure 1), the NCDS affects and shapes the northern sector of Mykonos Island (Avigad et al., 1998; Brichau et al., 2008; Lecomte et al., 2010; Lee & Lister, 1992; Menant et al., 2013) and represents the subject of the present work. In the study area, the NCDS shows a complex architecture, which is composed of two main branches namely the Livada ductile detachment and Mykonos brittle detachment that accommodated several kms of vertical (~ 12 km) and horizontal (~ 30 km) displacement (eg Brichau et al., 2008; Lecomte et al., 2010; Lee & Lister, 1992; Ring et al., 2010). The aim of the present work is to describe the spatial architecture of Livada and Mykonos structures and to give new insights into their mutual spatial relationships and their meaning in a regional scale view of NCDS. Moreover, we aim to define how deformation is partitioned

CONTACT Costantino Zuccari costantino.zuccari@dst.unipi.it Department of Earth Sciences, University of Pisa, Pisa 56126, Italy
Supplemental data for this article can be accessed online at https://doi.org/10.1080/17445647.2023.2277387.

into the footwall of the NCDS, where a thick and laterally continuous granitic pluton washighly deformed during the development of the NCDS. By providing new structural and a detailed geological map (see Main Map in the supplementary material) we provide new insights into the evolution of the NCDS and the related structures of the Livada and Mykonos branches.

2. Geological setting

The Cycladic Massif belongs to the Hellenides (eg Hejl et al., 2002; Papanikolaou, 2009, 2013), which is part of the Alpine orogenic belt and forms a roughly ~E-W trending orogen in the eastern Mediterranean region, following the curved shape of the active Hellenic Subduction zone in the southern Aegean (Figure 1(a); eg Jolivet & Brun, 2010; Ring & Layer, 2003). The Cretaceous-Oligocene evolution of the Hellenides (eg Jolivet et al., 2010; Jolivet & Faccenna, 2000; Lamont et al., 2023a, 2023b; Lecomte et al., 2010) resulted from the convergence between African and European plates that led to a pile of continental (Pelagonia and Apulia) and oceanic (Pindos and Vardar) units stacked during the subduction and collision phases (Figure 1(a); Aravadinou et al., 2022; Gerogiannis et al., 2022; Glodny & Ring, 2022; Jolivet & Faccenna, 2000; Lamont et al., 2023a, 2023b; Rosenbaum et al., 2002). From north to south (Figure 1(a)) those units encompass (i) the Rhodope – Sakarya Block, (ii) the Vardar-Izmir Oceanic Unit, forming the homonym suture zone in the north (eg Glodny & Ring, 2022; Ring et al., 2010), (iii) the continental Pelagonian Block, (iv) the Pindos Oceanic Block, and (v) the Tripolitza – Ionian Block, together forming the Apulian succession, overlain by Eocene-Oligocene flysch (eg Jolivet et al., 2010; Jolivet & Brun, 2010; Ring et al., 2010).

Rocks exposed in Mykonos Island belong to the Cycladic Massif (southern Aegean Sea, Figure 1(b)), which represents one of the southern offshoots of the Hellenides. The tectonostratigraphy of the Cycladic Massif can be divided into three main tectonic units (Figure 1(b)), which werestacked in the Eocene-Oligocene times (eg Ring et al., 2010; Seward et al., 2009; Skarpelis, 2002; Xypolias et al., 2012). From the structural base to the top, the sequence is mainly represented by (i) the Cycladic Basement unit (CBS), which forms the Variscan poly-metamorphosed crystalline complex of the Cycladic system (Figure 1(b); Jolivet & Brun, 2010; Keay, 1998; Laurent et al., 2015), (ii) the Cycladic Blueschist Unit (CBU), which likely represents the subducted and metamorphosed part of the Pindos Unit and experiencing both prograde and retrograde metamorphism (Aravadinou et al., 2022; Brady et al., 2004; Gerogiannis & Xypolias, 2017; Jolivet & Brun, 2010; Kotowski et al., 2022; Lamont et al., 2023a, 2023b; Ring et al., 2010), and (iii) the Upper Cycladic Unit (UCU), which represents a crystalline complex with rocks of continental and oceanic affinity affected by HT-metamorphism (eg Glodny & Ring, 2022; Lecomte et al., 2010; Martha et al., 2016; Papanikolaou, 2009).

The Cycladic Massif, and in particular the CBU, experienced a complex tectono-metamorphic evolution reaching eclogitic to blueschists facies conditions during the Late Cretaceous-Eocene time (eg Brady et al., 2004; Gerogiannis & Xypolias, 2017; Glodny & Ring, 2022; Jolivet & Brun, 2010; Lamont et al., 2023a, 2023b; Ring et al., 2010). These HP-LT conditions were progressively followed by lower-P conditions overprinting during the Oligocene and the early Miocene (eg Beaudoin et al., 2015; Bröcker et al., 2013; Glodny & Ring, 2022; Jolivet & Brun, 2010; Lamont et al., 2023a, 2023b; Ring et al., 2010). The Miocene overprinting phase is likely linked to the onset of the slab retreat-related back-arc extension, starting from ~ 35 Ma, and exhuming the CBU by cumulating tens and hundreds of kms of vertical and horizontal displacement, respectively (eg Brichau et al., 2007, 2010; Jolivet et al., 2010; Jolivet & Brun, 2010; Jolivet & Faccenna, 2000; Sànchez-Goméz et al., 2002). Alternatively, the exhumation of the HP-LT rocks has been related to a channel flow model along the subduction interface that allowed the activation of normal-sense detachments in a purely compressional environment (Searle & Lamont, 2022). However, the greater part of the exhumation and displacement along the detachments were cumulated during the Middle-Late Miocene. These detachments dip shallow towards North and South and are associated with top-to-the North and South shear sense, respectively (eg the North Cycladic Detachment System, NCDS; the Naxos – Paros Detachment System, NPDS; the West Cycladic Detachment System, WCDS; the South Cycladic Detachment System; Figure 1(b); Bakowsky et al., 2023; Coleman et al., 2019; Grasemann et al., 2012, 2018; Jolivet et al., 2010; Lamont et al., 2023b; Lee & Lister, 1992; Mehl et al., 2007; Rabillard et al., 2018; Ring et al., 2011). The back-arc extension was accompanied by the emplacement of syn-tectonic large Miocene granitic and monzogranitic bodies, which intruded the exhuming Units of the Cycladic Massif and shaped the actual setting of the Aegean Metamorphic Core Complex (MCC; Beaudoin et al., 2015; Cao et al., 2013; Jolivet et al., 2010; Jolivet & Brun, 2010; Lamont et al., 2023a, 2023b; Lecomte et al., 2010; Rabillard et al., 2018).

Mykonos Island (Figure 2(a)) represents a perfect location to study the relationships between the stacking of the different Cycladic units, extensional back-arc tectonics and syn-extensional Miocene granitic intrusion (Brichau et al., 2008; Lee & Lister, 1992; Menant et al., 2013). The northern sector of the island is interested by the Livada (LD) and the Mykonos

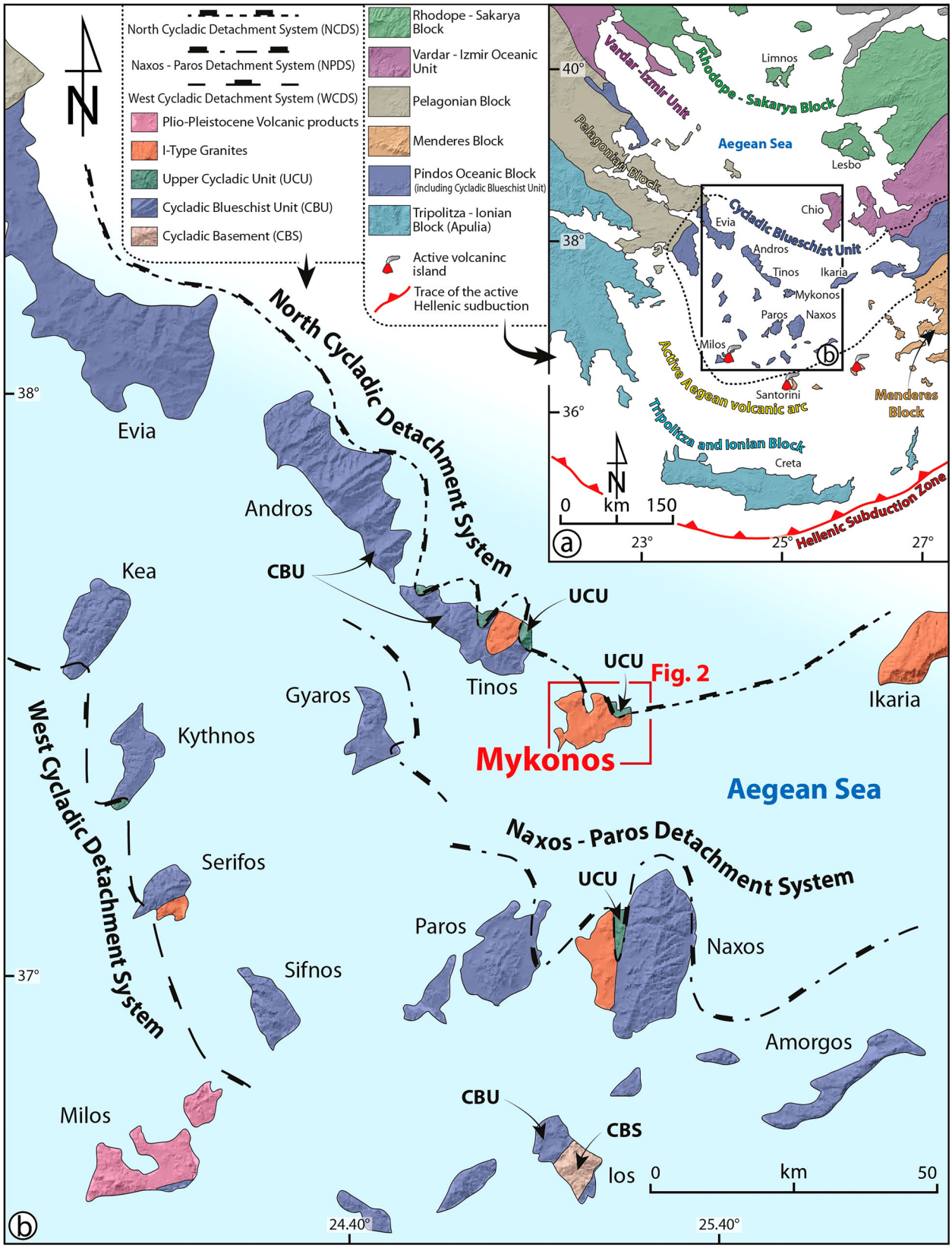

Figure 1. (a) Simplified tectonic map showing the major tectonic units in the Aegean region. (b) Schematic map of the western-central Cyclades. After Lecomte et al. (2010) and Lamont et al. (2023b).

(MD) detachments, which represent the ductile and brittle branches of the NCSD, respectively (Figure 2 (b); eg Brichau et al., 2007; Glodny & Ring, 2022; Jolivet et al., 2010). More in detail, the LD brings in contact the Miocene Mykonos Granite in the footwall with the Upper Cycladic Unit (metabasites) at the hanging wall (Figure 2(b); Brichau et al., 2006; Glodny & Ring, 2022; Jolivet et al., 2010; Lecomte et al., 2010). In the western part of the mapped area (ie Mersini beach locality; Main Map) the LD spectacularly

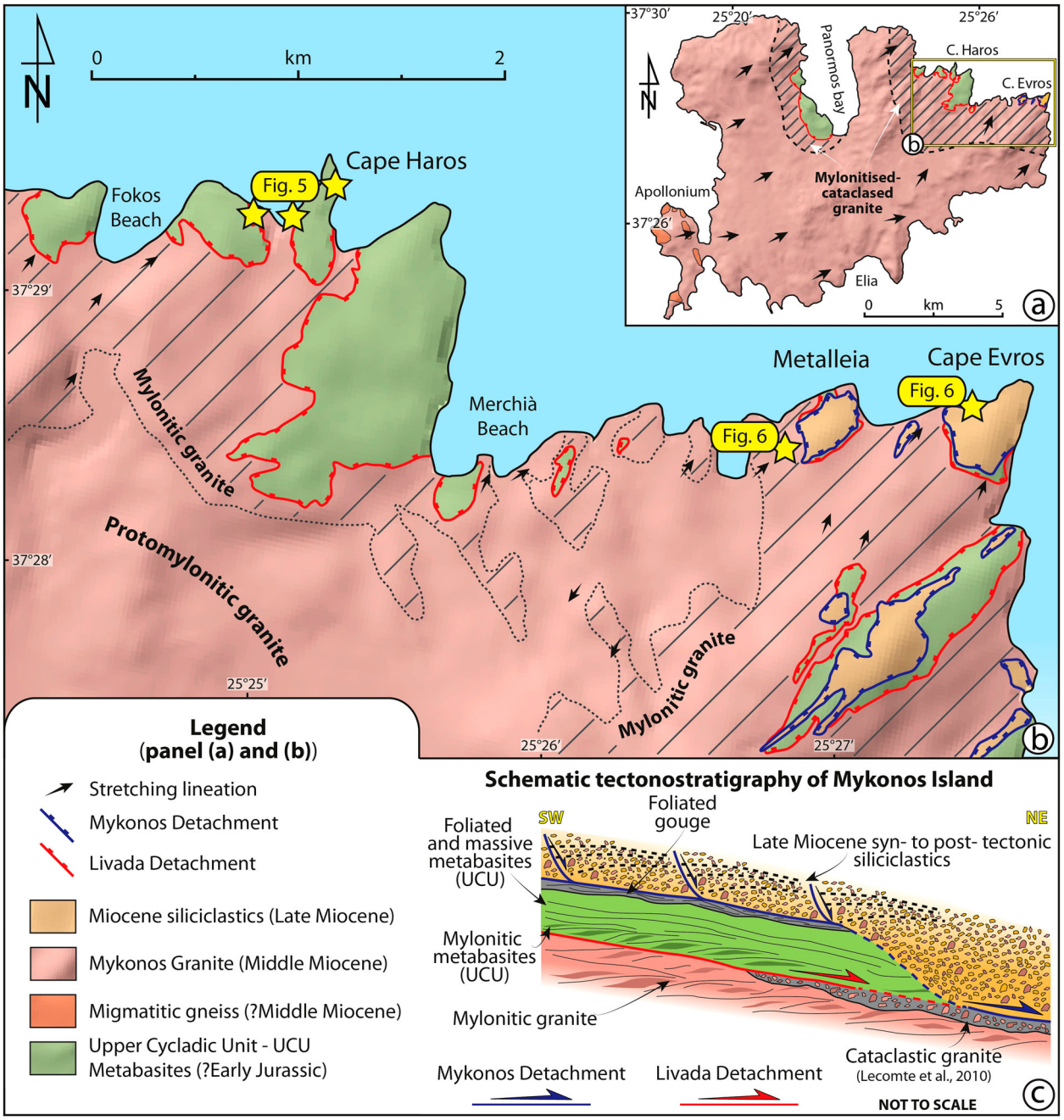

Figure 2. (a) Simplified geological map of Mykonos Island (modified from Lecomte et al., 2010). (b) Schematic geological map of the northeastern sector of Mykonos Island resulted from our study (see also the Main Map in the supplementary material), highlighting the geometrical relationships between the Mykonos and Livada Detachments and the heterogeneous distribution of mylonitisation. (c) Tectonostratigraphy of Mykonos Island in the analysed sector.

crops out, bringing in contact the Mykonos Granite (with a monzogranitic composition) in the footwall with the Metabasites in the hanging wall, which is composed of a thick mylonitic shear zone developed within the metabasites and locally transposing the aplitic sills and dykes (eg Menant et al., 2013), which are then in turn cut by a dense network of late high angle normal faults. Depending on the sector of the island, the MD puts in contact the Upper Cycladic Unit (Metabasites) in the footwall with the Miocene siliciclastics in the hanging wall (western sector; see Main Map in the supplementary material), or, due to the tectonic elision, the Miocene Siliciclastics rest in tectonic contact directly on the Miocene Mykonos Granite (easter sector; Figure 2 (b); Main Map). The latter feature is also particularly evident in Panormos Bay (not represented in the Main Map), where the hydrothermalised granite in the footwall is overlain by the Miocene Siliciclastic due to the complete tectonic elision of the Metabasites (eg Lecomte et al., 2010; Menant et al., 2013). Locally, where directly in contact with the Miocene Siliciclastics in the hanging wall, the granite is affected by a strong fracturing and cataclasis (Figure 2(c)), attesting also to the progressive cooling of the system during the unroofing and exhumation of the

pluton that also allowed the transition from the ductile LD to the brittle MD.

3. Methods

Geological mapping was carried out by using the topographic base map extrapolated from the Digital Elevation Model (DEM; courtesy of the Institute of Geology and Mineral Exploration of Athens), at 1:8000, 1:3000 and 1:2500 scales, depending on the necessary detail to elucidate the main structural features of the studied sector. To be more accurate during the fieldwork topographic map and satellite images (Google Earth® base) were overlapped. The spatial reference of the Cartesian grid and coordinates is based on the metric system WGS 84/UTM zone 35N (EPSG: 32635).

To describe the spatial distribution of different units and their relationships with the main faults and shear zones, a detailed structural analysis was made on key exposures throughout the study area. To characterise and reconstruct the architectural features of the deformed units, we systematically collected and mapped: (i) primary (eg magmatic) and secondary (tectonic) foliation, (ii) fault planes, (iii) stretching lineation and slickenlines, and (iv) bedding of the sedimentary units. All planar data were recorded according to the dip direction/dip angle convention, whereas linear measurements according to the trend/plunge convention. Data were processed, plotted, and analysed using the *Stereonet* software (version 11.3.0).

To document the partitioning of deformation and the spatial distribution of different fabric variations in grain size and microstructures were mapped. Specifically, four exposed units were differentiated in the Main Map (see the supplementary material) as follows, from the structural base toward the top of the sequence:

1. Mykonos Granite: (i) magmatic fabric, (ii) protomylonitic granite, (iii) mylonitic and ultramylonitic granite;
2. Aplite, mapped as a zone interested by pervasive intrusions of aplitic dikes and sills;
3. Upper Cycladic Unit: (i) massive metabasites and (ii) hydrothermalised metabasites;
4. Miocene Siliciclastics: (i) sedimentary-chaotic breccia and (ii) stratified sediments.

The Main Map (1:8000 scale) thus reports this differentiation and provides new data on the onset and partitioning of deformation within the Mykonos Granite in the footwall of the NCDS. This differentiation is also useful to discriminate the relationship between the position of the MD and the LD, the development of different mylonitic fabrics, and the mapped fluid-related structures. It represents the base for further and more detailed investigations.

4. Data and results

4.1. Lithological units

In this section, we describe the composition and internal structure of the units exposed in the analysed sector. We also provide specific information for each unit that are useful to their recognition and mapping in the field.

***Mykonos Granite* – (Go, Gp, Gm)** (Serravallian). The unit covers the whole southern part of the study area (Figure 2(a,b); Main Map). The mineralogical composition is variable, spanning from syenogranitic to monzogranitic, and it is represented by K-feldspar and plagioclase phenocrysts within a fine-grained biotite and quartz matrix. The magmatic fabric (Gm abbreviation in Main Map; Figure 3(a)) is locally preserved with K-feldspar phenocrysts (up to 7–8 cm) with shape-preferred orientation. Locally an incipient magmatic lineation is preserved and represented by elongated-isoriented K-feldspar and quartz grains. In most part of the study area, the magmatic fabric is partially or completely obliterated by a ductile proto – to mylonitic fabric (Gp and Gm abbreviations, Main Map; Figure 3(a)). The intensity of deformation seems to not be exclusively related to the proximity with respect to the Livada and Mykonos Detachments, where mylonitic to ultramylonitic granite crops out even far (more than 300 m) from the main detachment zones (Figure 2(a,b); Main Map). Mylonitic rocks are characterized by a pervasive stretching lineation defined by elongated isoriented K-feldspars crystals and polycrystalline quartz ribbons, and display kinematic indicators represented by K-feldspar and quartz porphyroclasts, often with asymmetric tails made of fine-grained recrystallised quartz. In the mapped area it is exposed the top of the Mykonos Granite, whereas unfortunately the base of the pluton is only exposed in the western part of the Island. By considering the granite exposed and reported in the main map, the thickness of the unit reasonably exceeds 500 m (Geological cross sections – Main Map).

***Upper Cycladic Unit – Metabasites* – Mm, Mh** ((?)Early Jurassic). This Unit is represented by light to dark green and blackish metabasites (Figure 2; Figure 3(b); Mm abbreviation; Main Map, supplementary material) interposed between the Livada and Mykonos detachments (Figure 2(c); Main Map). In the eastern part of the study area, they are only preserved as small patches (eg Cape Evros and Metalleia localities, Main Map). Due to their low preservation, their internal structure is not easily recognisable

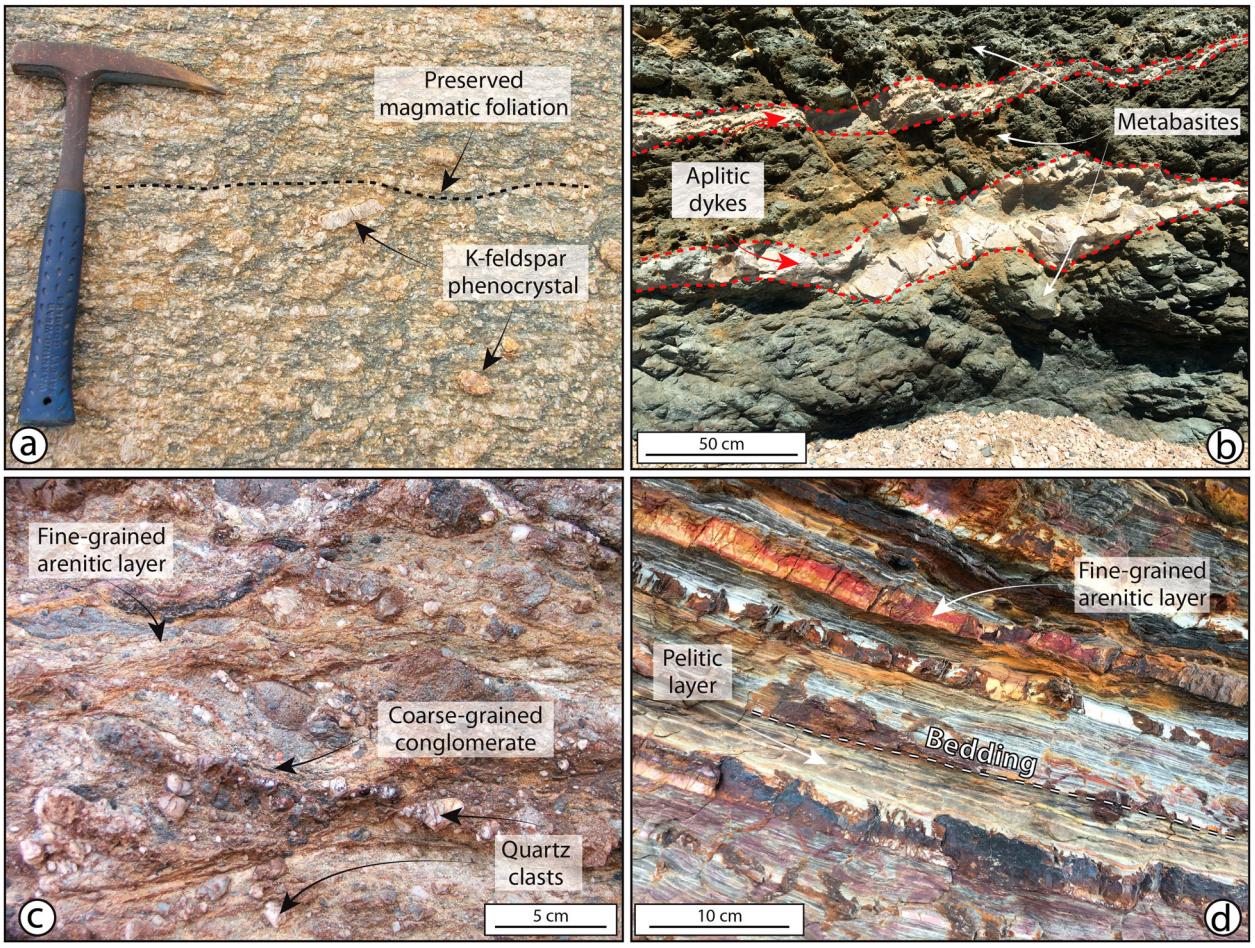

Figure 3. Main lithological units outcropping in the northeastern sector of Mykonos Island. (a) Granite preserving the original magmatic foliation and euhedral to sub-euhedral feldspar crystals. (b) Green to blackish metabasites, belonging to the Upper Cycladic Unit (UCU), cut and dissected by multiple heteromeric white aplitic dykes. (c) Coarse-grained conglomerates of the lower portion of the Miocene siliciclastics. (d) Pelitic and fine-grained arenitic layers of the upper portion of the Miocene Siliciclastics.

throughout the mapped sector. In general, however, metabasites are massive (Mm abbreviation; Main Map; Figure 3(b)) in the portions away from the detachments, whereas they become pervasively foliated approaching the LD and MD. The original fabric is completely obliterated approaching the Mykonos Detachment, where metabasites are often hydrothermally altered (Mh abbreviation, Main Map), brecciated and cut by a pervasive network of hydrothermal Fe-oxides and barite veins (eg Menant et al., 2013). Locally metabasites are intruded and cut by multiscale (from 10 to 50 cm thick) white to grey aplitic dykes (Figure 3(b)). The maximum thickness of the units does not exceed ≈10–60 m above the LD (Main Map).

***Miocene Siliciclastics* – Sb, Ss** (Late Miocene). The siliciclastic sedimentary Miocene unit crops out as localised patches above the MD (Figure 2(b)) and is represented by two different sedimentary facies (Figure 3(c-d)). The basal facies (Sb abbreviation, Main Map) consists of variably thick and laterally discontinuous polymictic and poorly sorted conglomeratic and breccia lenses, at times interlayered with thin and laminated fine-grained arenitic layers that increase upwards (Figure 3(c)). The uppermost facies (Ss abbreviation, Main Map) consists of grey, yellow and reddish siltstones and sandstones (Figure 3(d)), where the pelitic portion represents the principal component. Both facies are cut and dissected by low-spaced and multiscale syn-sedimentary faults and display pervasive syn-tectonic structures. The thickness of the entire unit is variable throughout the area but in general spans from 10 to 40 m (Main Map).

***Quaternary deposits* – Q** (abbreviation in Main Map). The Quaternary deposits are mainly exposed in the northeasternmost sector of the map, near Cape Evros and Metalleia localities (Main Map). They are represented by yellow calcarenites with cross-bedded lamination containing rare lenses of matrix-supported conglomerates. Locally the quaternary deposits are also composed of fine-grained and evolved sandstones described as eolianites and recognised with the traditional name of 'Poros' (eg Desruelles et al., 2009; Varti-Mataranga & Piper, 2004). They form terraces in depressed areas with a total thickness that rarely reaches ≈20 m.

4.2. Structural setting

The LD and MD are spectacularly exposed in the northernmost part of the study area along three main sections from east to west: (i) Cape Evros, (ii) Metalleia and (iii) Cape Haros (Figure 2(a,b); Main Map). Both branches of the NCDS exposed in these sections are described in the following sections. The Cape Evros section includes the Metalleia area (Main Map). The stereographic projection of structural data (eg foliations, stretching lineations, slickenlines, orientations of the fault and shear zone surfaces) for the study area is reported in Figure 4.

4.2.1. The Cape Haros section

The ductile shear zone of the LD is exposed in Cape Haros, and juxtaposes the Mykonos Granite, in the footwall, with several tens of meters (at least 50 m) thick metabasites of the Upper Cycladic Units, in the hanging wall (Figure 5(a,b); Main Map). Locally, the LD shear zone shows evidence of brittle deformation, accompanied by the formation of NE-dipping subsidiary slip surfaces showing a top-to-the NE sense of shearing, thus concordant with the tectonic transport registered by the later brittle phase. Ductile deformation localises both in the granite and in metabasites, which display a general NE-dipping mylonitic foliation (Figures 4(a–c) and 5(a,b)). The metabasites are foliated with thinly spaced foliation, whereas the granite displays a more spaced and less pervasive foliation (Figures 4e and 5(b)). Ductile deformation characterises indeed only a few meters (10–15 m) of metabasites above the main detachment zone, whereas in the granite the foliated zone reaches up to 500 m (Figure 5(a)). The mylonitic foliation of both granite and metabasites strikes NW-SE whereas the stretching lineation is defined by polycrystalline aggregates of quartz (trending N045° to N070° and dipping shallowly to the NE; Figures 4(b) and 5(a)). Kinematic indicators such as σ-type porphyroclasts and SC fabrics in the granite are consistent with a top-to-the NNE sense of shear along the LD. Approaching to the LD, foliation becomes more pervasive within the granite, exhibiting an ultramylonitic fabric dipping shallowly to the NE (Figures 4(a,c) and 5(c,d)). However, the mylonitic fabric in the granite is not homogenously distributed in the footwall of the LD. The ultramylonitic fabric is indeed localised within centimetric or decimetric mylonitic (Figure 5(d)) domains, whereas the surrounding mylonitic granite shows only protomylonitic fabric, thus confirming a strong localisation of the strain into narrow domains (Figure 5(c, d)). This strong localisation is also confirmed by the presence of even preserved magmatic original fabrics (Figure 5(c)) in contact with ultramylonitic domains, which are thus able to accommodate most part of the deformation.

At Cape Haros the MD is only exposed in a site, in which the Miocene Siliciclastics are in contact with the metabasites of the Upper Cycladic Unit (Figure 5 (e-f)). In this site, the MD is represented by a complex fault zone (Figure 5(e,f)) composed of a thick (up to 2 m) foliated domain with SC structures showing NE-directed shearing (Figure 4; Figure 5(e,f)) and a 30–40 cm thick foliated, partially cohesive gouge, also showing top-to-the NE shear sense (Figure 5(f)). The conglomerates in the hanging wall show evidence of syn-sedimentary brittle tectonics, generally represented by high-angle normal faults that root within the main SC MD fault zone. In the footwall block, the metabasites show a pervasive hydrothermal alteration (Figure 5 (b,e)) that increases toward the main fault plane. Metabasites are in general poorly preserved (Figure 5(e)) but locally show SCC' domains consistent with the regional top-to-the NE sense of shear.

4.2.2. The Cape Evros section

The LD is not well preserved in Cape Evros, where metabasites of the Upper Cycladic Units occur as small patches with a poor lateral continuity (or are even completely elided), bounded to the top and the bottom by the MD and the LD, respectively (Figure 6(a)). As for other portions of the northern sector of Mykonos Island, the Metabasites were embedded and transposed within the upper part of the Mykonos Granite during the development of the LD. However, where metabasites crop out, they are characterised by a well-developed mylonitic foliation that at times composes asymmetrical folds showing NE vergence, concordant with those described for the LD in the Cape Haros granite and for the whole Cape Haros section. Compared to the Cape Haros section, ductile deformation in the Cape Evros section (Metalleia locality, Panel B in the Main Map; Figure 2) is more homogeneous and partitioned, and the whole granite is interested by thick mylonitic domains that reach even several tens of decimeters and meters (Figure 6(c,d)). With respect to those described for Cape Haros, in Cape Evros section magmatic fabric and localised ultramylonitic centimetric domains are completely absent, thus revealing a more partitioned strain and pervasive deformation within thicker granite volumes. Moreover, the mylonitic foliation and stretching lineations within the granite that crops out in Cape Evros and in the surrounding areas (eg Metalleia locality, Panel B in the Main Map) show a few variations in dip, trend, and plunge (Main Map, geological cross-section E-F) that can be related to both the pervasive and later extensional tectonic (related to the MD activity) and to the strike-slip compressional regimes that affected the area after the formation of the LD (eg Menant et al., 2013).

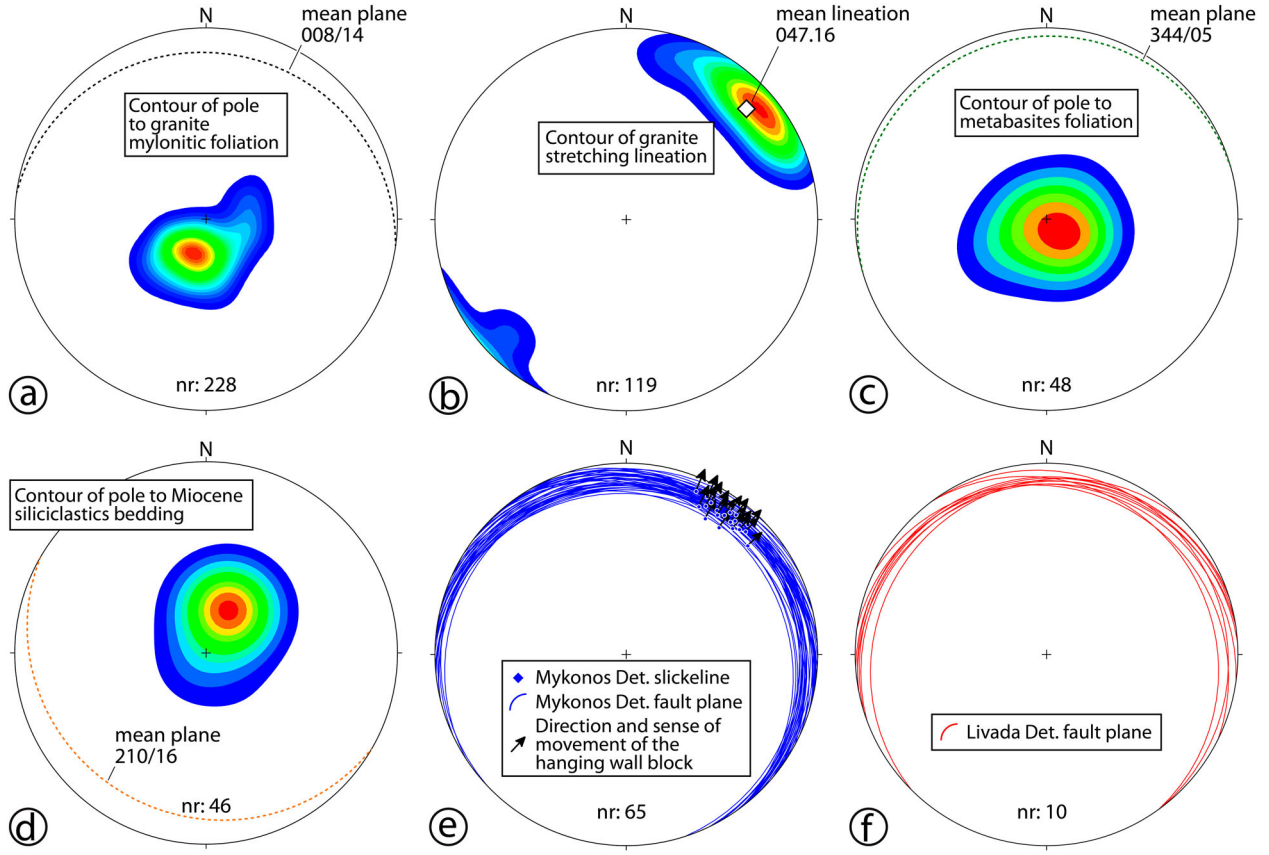

Figure 4. Stereographic projections (Schmidt net, lower hemisphere) of the measured structural elements. (a) Contour of poles to the mylonitic foliation in the granite. (b) Contour of stretching lineations associated with the mylonitic foliation in the granite. (c) Contour of poles to the foliation in the metabasites. (d) Contour of poles to the bedding of the Miocene siliciclastics. (e) Mykonos Detachment fault plane and associated slicknelines. (f) Livada detachment fault planes associated with the ductile shear zone. Kamb contours with interval = 3 and significance level = 2.

The MD is spectacularly exposed in Cape Evros (Panel A, Main Map), where it juxtaposes the Miocene Siliciclastics with the metabasites of the Upper Cycladic Unit or directly with the Mykonos Granite, if metabasites are missing (Figure 2(b,e); Main Map). In the footwall of the MD, metabasites are generally characterised by a pervasive foliation (Figures 4(c) and 6(a,b)) that is abruptly cut, at the top, by laterally discontinuous hydrothermalised cataclastic bodies (Figure 6(b)), altered and intersected by a dense network of Fe-oxides and barite veins (Figure 6(b)). These cataclastic domains are bounded at the top by the Fe-oxides mineralised sharp surface of the Mykonos Detachment (Figure 6(a,b)), which dips shallowly toward the NE and is marked by NE-plunging dip-slip slickenlines (Figure 4(e)). Moreover, the principal fault zone of the MD is marked by laterally discontinuous and variably thick (up to ~ 30 cm) gouge lenses and cataclastic domains formed at the expense of both metabasites and Miocene Siliciclastics (Figure 6(e,f)). Locally the main MD plane is decorated by discontinuous polychrome lenses of poorly cemented fault gouge (Figure 6(f)), which reaches a few decimetres in thickness and generally does not display evidence of an internal organisation. Deformation above the gouge is accommodated by a dense network of conjugate syn-sedimentary NW-SE striking normal faults that cut across the Miocene Siliciclastics, which in turn show growth strata and geometries within the pelitic and fine-grained layers that rest directly on the faults (Figure 6(e)). Subsidiary syn-sedimentary faults root into the MD main fault plane and into subsidiary dècollement surfaces, subparallel with respect to the principal MD showing a general sense of shear towards the NE (Figure 6(e)).

5. Discussion and conclusions

The presented geological map (Main Map, supplementary material) describes the complex architecture of a portion of the North Cycladic Detachment System exposed in the northeastern part of Mykonos Island, where it is defined by the Livada (ductile-brittle) and Mykonos (brittle) branches. By integrating geological mapping of different tectono-stratigraphic units, the ductile fabrics that characterise the granite, and structural analysis on key exposures (ie Cape Evros, Metalleia and Cape Haros), we expand our knowledge for the structural setting of Mykonos Island and report new data on the deformation related to the post-orogenic evolution in Aegean Region. The analysis of the architecture of the Mykonos and

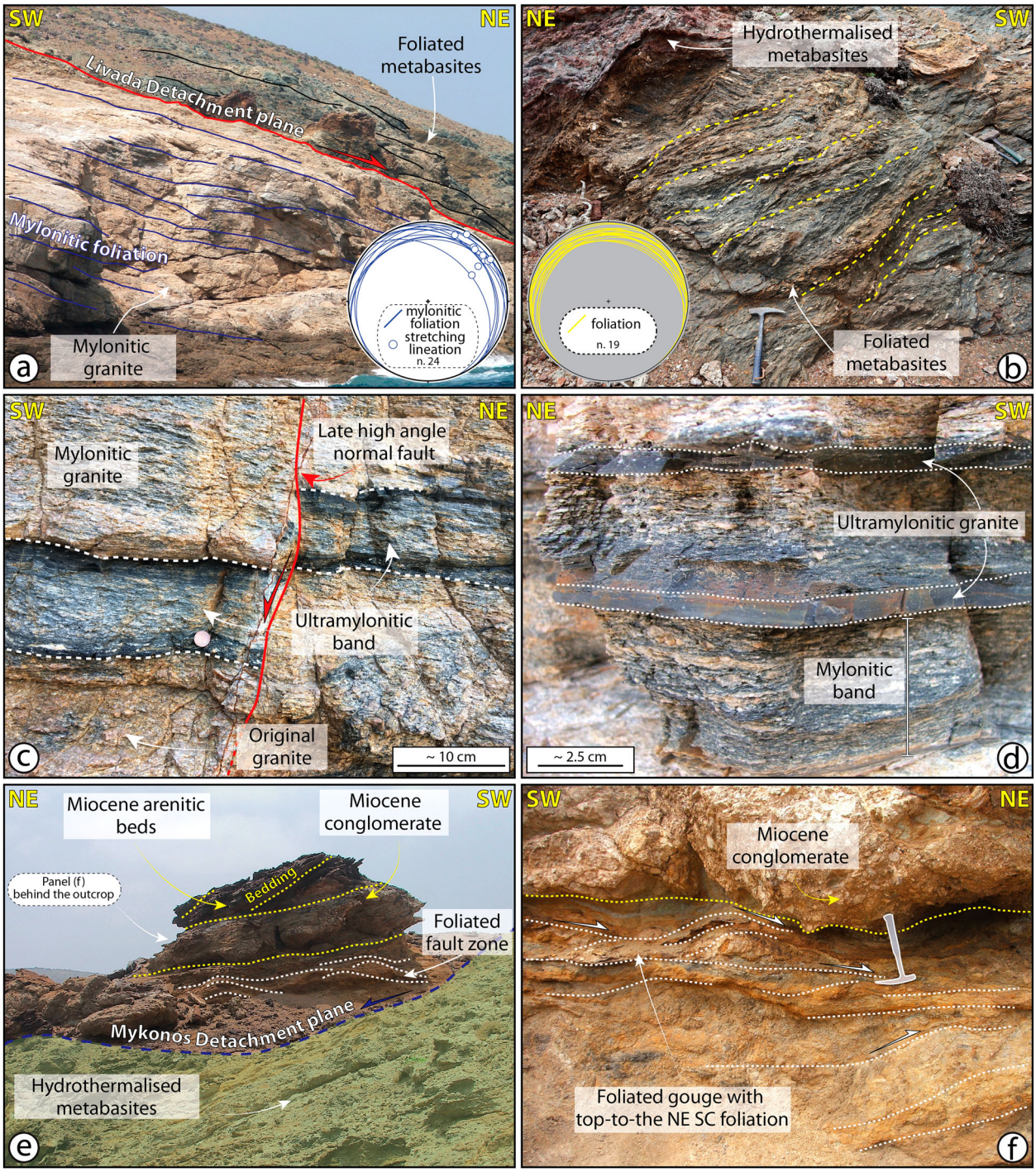

Figure 5. (a) Exposure of the Livada Detachment in Cape Haros and contact between the mylonitic granite and the foliated metabasites of the UCU. (b) Detail of the pervasive N-dipping foliation within the hydrothermalised metabasites in the hanging wall of the Livada Detachment. (c) Mylonitic and ultramylonitic banding with partially preserved original granite. (d) Interlayered mylonitic and ultramylonitic granite. (e) Exposure of the Mykonos Detachment in Cape Haros locality and contact between the Miocene Siliclastics and the metabasites of the UCU. (f) Detail of the Mykonos Detachment with a foliated gouge and a top-to-the NE associated SC foliation.

Livada detachments allows, thus, the following considerations:

(i) The mapping of the Mykonos Detachment along strike (ie ~E-W in northeastern Mykonos Island) shows that deformation proceeds through different processes. In Cape Evros deformation is strongly localised along a narrow fault zone with respect to the Haros locality. The deformation seems to be localised, at least during a late stage of the fault evolution, along a main and sharp slip surface, which is also characterised by a pervasive barite – and iron oxides-rich mineralisation (Figure 6). Even if several gouges decorate the fault zone, they are only represented by localised and poorly laterally continuous pockets of plastic and foliated material. On the other hand, in Cape Haros, the MD fault zone is

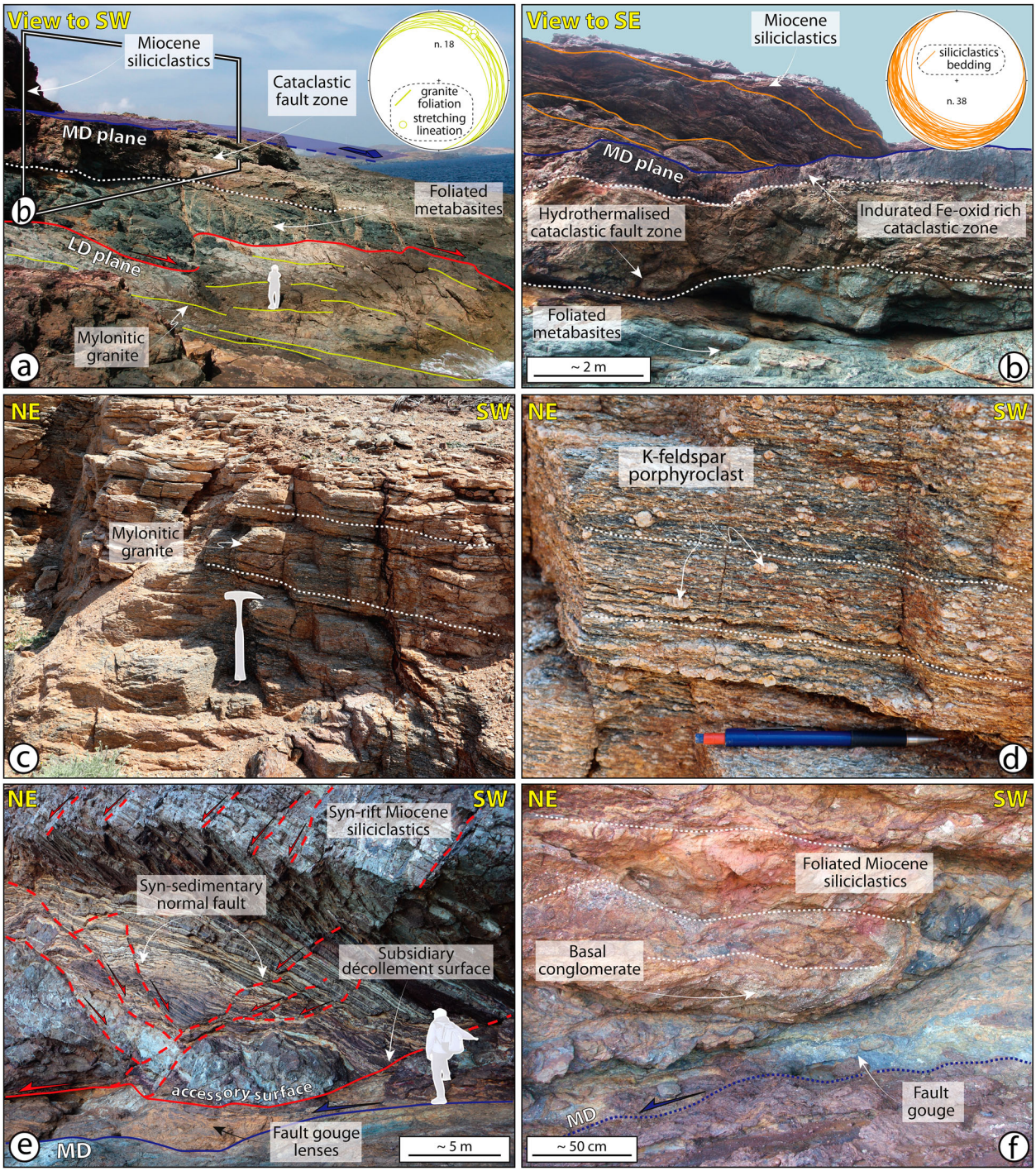

Figure 6. (a) Exposure of the Livada (LD) and Mykonos (MD) detachments in Cape Evros locality, where only small lenses of foliated metabasites are preserved between the granite and the Miocene siliclastics. The position of the panel (b) is shown. (b) Detail of the Mykonos detachment and of the associated hydrothermalised cataclastic fault zone. (c) Mylonitic granite in the Metalleia locality (Cape Evros area; see the Main Map in the supplementary material). (d) Detail of the mylonitic foliation in the granite with elongated sigmoidal K-feldspar porphyroclast. Syn-sedimentary high angle normal fault dissecting the syn-rift Miocene siliciclastic in the hanging wall of the Mykonos Detachment. (f) Detail of the polychrome gouge lenses along the main Mykonos Detachment.

formed by a thick SC foliated domain, which is in turn characterised by multiple foliated gouge layers (Figure 5). The displacement is there accommodated by a thick volume of fault rocks with respect to those described for Cape Evros, that, together with the absence of a main slip surface (Figure 5) suggest a strong deformation partitioning in Cape Haros.

(ii) The analysis of the spatial distribution of the Metabasites of the Upper Cycladic Unit highlighted that the MD and LD are not completely parallel each other along the dip (Main Map). As it is also reported in the geological cross-sections G-H and I-L, in which both LD and MD are represented, the development of the brittle MD locally induces the complete elision

of the Metabasites that are, also, at times preserved as slices within the mylonitic foliation related to the ductile history of the Livada (geological cross-section I-L).

(iii) Although in literature has been reported that fabric in the Mykonos Granite evolves from proto – to mylonitic moving from SW to NE (eg Denèle et al., 2011) as well as that this fabric should be related to the proximity with respect to the LD and MD, the detailed mapping of the spatial distribution of different fabrics in the granite highlights that the deformation in the Mykonos Granite displays a more complex pattern. Monzogranite in Cape Haros, in the footwall of the LD, shows a strong strain localisation, which is characterised by the development of localised mylonitic to ultra-mylonitic domains which pass to proto-mylonitic fabric or even to the original magmatic fabric in a few centimetres or decimetres (Figure 5(c,d)). On the other hand, in Cape Evros, where the composition of the granite is more leucocratic, the strain is generally more partitioned within thicker rock volumes characterised by homogeneous fabrics, which only locally reach the ultra-mylonitic development and where the original magmatic fabric is completely obliterated, thus suggesting a less pronounced partitioning of the strain during the development of the LD.

In conclusion, our results offer a refinement of the knowledge of the architecture of the sector of the NCDS exposed in Mykonos Island and of the distribution of the associated deformation structures, both in the footwall and in the hanging wall of the Livada and Mykonos detachments. The presented data in particular suggest that the ductile deformation related to the LD differs from West (Cape Haros) to the East (Cape Evros), where the different grade of strain localisation seems to be related to the original composition of the granite, which pass from monzogranitic – to leucocratic-dominated moving toward west.

Concerning the brittle history of the NCDS in Mykonos, the presented data show that the development of the Mykonos Detachment does not completely follow the former original setting of the Livada Detachment, being not parallel to the former ductile shear zone. The consideration of the architectural development of the LD and MD, suggest that this different trending of the structures could have allowed (i) the partial or complete elision of the metabasites in the hanging wall and in the footwall of the LD and MD, respectively, and (ii) the beginning of cataclasis and brittle deformation in the granite where the metabasites are completely elided.

Even if these findings are related to the development of the detachments in the Mykonos Island, our data could also shed new data on the evolution of a MCC during the progressive exhumation of a pluton, that can be accompanied by the formation of multiple detachments (brittle and ductile) as in Mykonos, and not by the evolution of a single detachment that progressively passes from ductile, warmer and deeper, to brittle, cooler and shallower deformation conditions.

Software

The map was digitalised and georeferenced with the open-source software Qgis (version 2.18.13, 'Las Palmas' version, https://www.qgis.org/it/site/). Final editing of the map and the geological cross sections was realised with Adobe Illustrator (version CC). Stereographic projections were realised using the software Stereonet 11 (version 11.0.7, http://www.geo.cornell.edu/geology/faculty/RWA/programs/stereonet.html).

Acknowledgements

We want to thank the reviewers Prof. Rodolfo Carosi, Prof. Laurent Jolivet and Dr. Jiří Pánek for their constructive comments and suggestions and the Associate Editor Claudio Riccomini for the editorial handling.

Disclosure statement

No potential conflict of interest was reported by the author(s).

Funding

This research was made possible by financial support from the PRIN 2020_FAST project (Fault Architecture in Space and Time; PI: Giulio Viola, University of Bologna, Italy), a research project funded by the Italian Ministry for University and Research (MUR) with the PRIN 2020 funding action (CUP: J33C22000170001).

Data availability statement

The authors confirm that the data supporting the findings of this study are available within the article and its supplementary materials.

References

Agostini, S., Doglioni, C., Innocenti, F., Manetti, P., & Tonarini, S. (2010). On the geodynamics of the Aegean rift. *Tectonophysics*, *488*(1–4), 7–21. https://doi.org/10.1016/j.tecto.2009.07.025

Aravadinou, E., Gerogiannis, N., & Xypolias, P. (2022). Development and passive exhumation of high-pressure shear zones (Blueschist Unit, Syros): Insights from quartz and columnar calcite microstructures. *Journal of Structural Geology*, *159*, 104607. https://doi.org/10.1016/j.jsg.2022.104607

Avigad, D., Baer, G., & Heimann, A. (1998). Block rotations and continental extension in the central Aegean Sea: Palaeomagnetic and structural evidence from Tinos and

Mykonos (Cyclades, Greece). *Earth and Planetary Science Letters*, *157*(1–2), 23–40. https://doi.org/10.1016/S0012-821X(98)00024-7

Bakowsky, C., Schneider, D. A., Grasemann, B., & Soukis, K. (2023). Miocene ductile thinning below the Folegandros Detachment System, Cyclades, Greece. *Terra Nova*. https://doi.org/10.1111/ter.12646

Beaudoin, A., Augier, R., Laurent, V., Jolivet, L., Lahfid, A., Bosse, V., Arbaret, L., Rabillard, A., & Menant, A. (2015). The ikaria high-temperature metamorphic core complex (Cyclades, Greece): Geometry, kinematics and thermal structure. *Journal of Geodynamics*, *92*, 18–41. https://doi.org/10.1016/J.JOG.2015.09.004

Brady, J. B., Markley, M. J., Schumacher, J. C., Cheney, J. T., & Bianciardi, G. A. (2004). Aragonite pseudomorphs in high-pressure marbles of Syros, Greece. *Journal of Structural Geology*, *26*(1), 3–9. https://doi.org/10.1016/S0191-8141(03)00099-3

Brichau, S., Ring, U., Carter, A., Bolhar, R., Monié, P., Stockli, D., & Brunel, M. (2008). Timing, slip rate, displacement and cooling history of the Mykonos detachment footwall, Cyclades, Greece, and implications for the opening of the Aegean Sea basin. *Journal of the Geological Society*, *165*(1), 263–277. https://doi.org/10.1144/0016-76492006-145

Brichau, S., Ring, U., Carter, A., Monié, P., Bolhar, R., Stockli, D., & Brunel, M. (2007). Extensional faulting on Tinos Island, Aegean Sea, Greece: How many detachments? *Tectonics*, *26*(4), 4. https://doi.org/10.1029/2006TC001969

Brichau, S., Ring, U., Ketcham, R. A., Carter, A., Stockli, D., & Brunel, M. (2006). Constraining the long-term evolution of the slip rate for a major extensional fault system in the central Aegean, Greece, using thermochronology. *Earth and Planetary Science Letters*, *241*(1–2), 293–306. https://doi.org/10.1016/j.epsl.2005.09.065

Brichau, S., Thomson, S., & Ring, U. (2010). Thermochronometric constraints on the tectonic evolution of the serifos detachment, Aegean Sea, Greece. *International Journal of Earth Sciences*, *99*(2), 379–393. https://doi.org/10.1007/s00531-008-0386-0

Bröcker, M., Baldwin, S., & Arkudas, R. (2013). The geological significance of 40Ar/39Ar and Rb–Sr white mica ages from Syros and Sifnos, Greece: A record of continuous (re)crystallization during exhumation? *Journal of Metamorphic Geology*, *31*(6), 629–646. https://doi.org/10.1111/jmg.12037

Cao, S., Neubauer, F., Bernroider, M., & Liu, J. (2013). The lateral boundary of a metamorphic core complex: The moutsounas shear zone on Naxos, Cyclades, Greece. *Journal of Structural Geology*, *54*, 103–128. https://doi.org/10.1016/j.jsg.2013.07.002

Coleman, M., Dubosq, R., Schneider, D. A., Grasemann, B., & Soukis, K. (2019). Along-strike consistency of an extensional detachment system, west Cyclades, Greece. *Terra Nova*, *31*(3), 220–233. https://doi.org/10.1111/ter.12388

Denèle, Y., Lecomte, E., Jolivet, L., Lacombe, O., Labrousse, L., Huet, B., & Le Pourhiet, L. (2011). Granite intrusion in a metamorphic core complex: The example of the Mykonos laccolith (Cyclades, Greece). *Tectonophysics*, *501*(1–4), 52–70. https://doi.org/10.1016/j.tecto.2011.01.013

Desruelles, S., Fouache, É, Ciner, A., Dalongeville, R., Pavlopoulos, K., Kosun, E., Coquinot, Y., & Potdevin, J. L. (2009). Beachrocks and sea level changes since Middle Holocene: Comparison between the insular group of Mykonos–Delos–Rhenia (Cyclades, Greece) and the southern coast of Turkey. *Global and Planetary Change*, *66*(1-2), 19–33. https://doi.org/10.1016/j.gloplacha.2008.07.009

Faure, M., Bonneau, M., & Pons, J. (1991). Ductile deformation and syntectonic granite emplacement during the late Miocene extension of the Aegea (Greece). *Bulletin de la Société Géologique de France*, *162*(1), 3–11. https://doi.org/10.2113/gssgfbull.162.1.3

Gerogiannis, N., Chatzaras, V., Aravadinou, E., Gürer, D., & Xypolias, P. (2022). Microstructural and textural modification of columnar calcite under increasing shear strain (Evia Island, Greece). *Journal of Structural Geology*, *160*, 104632. https://doi.org/10.1016/j.jsg.2022.104632

Gerogiannis, N., & Xypolias, P. (2017). Retroward extrusion of high-pressure rocks: An example from the Hellenides (Pelion Blueschist Nappe, NW Aegean). *Terra Nova*, *29*(6), 372–381. https://doi.org/10.1111/ter.12297

Glodny, J., & Ring, U. (2022). The Cycladic Blueschist Unit of the Hellenic subduction orogen: Protracted high-pressure metamorphism, decompression and reimbrication of a diachronous nappe stack. *Earth-Science Reviews*, *224*, 103883. https://doi.org/10.1016/j.earscirev.2021.103883

Grasemann, B., Huet, B., Schneider, D. A., Rice, A. H. N., Lemonnier, N., & Tschegg, C. (2018). Miocene postorogenic extension of the eocene synorogenic imbricated hellenic subduction channel: New constraints from milos (Cyclades, Greece). *GSA Bulletin*, *130*(1-2), 238–262. https://doi.org/10.1130/B31731.1

Grasemann, B., Schneider, D. A., Stöckli, D. F., & Iglseder, C. (2012). Miocene bivergent crustal extension in the Aegean: Evidence from the western Cyclades (Greece). *Lithosphere*, *4*(1), 23–39. https://doi.org/10.1130/L164.1

Hejl, E., Riedl, H., & Weingartner, H. (2002). Post-plutonic unroofing and morphogenesis of the Attic-Cycladic complex (Aegea, Greece). *Tectonophysics*, *349*(1-4), 37–56. https://doi.org/10.1016/S0040-1951(02)00045-8

Jolivet, L., & Brun, J. P. (2010). Cenozoic geodynamic evolution of the Aegean. *International Journal of Earth Sciences*, *99*(1), 109–138. https://doi.org/10.1007/s00531-008-0366-4

Jolivet, L., & Faccenna, C. (2000). Mediterranean extension and the Africa-Eurasia collision. *Tectonics*, *19*(6), 1095–1106. https://doi.org/10.1029/2000TC900018

Jolivet, L., Faccenna, C., Huet, B., Labrousse, L., Le Pourhiet, L., Lacombe, O., Lecomte, E., Burov, E., Denèle, Y., Brun, J. P., Philippon, M., Paul, A., Salaün, G., Karabulut, H., Piromallo, C., Monié, P., Gueydan, F., Okay, A. I., Oberhänsli, R., … , & Driussi, O. (2013). Aegean tectonics: Strain localisation, slab tearing and trench retreat. *Tectonophysics*, *597-598*, 1–33. https://doi.org/10.1016/j.tecto.2012.06.011

Jolivet, L., Lecomte, E., Huet, B., Denèle, Y., Lacombe, O., Labrousse, L., Le Pourhiet, L., & Mehl, C. (2010). The North Cycladic Detachment System. *Earth and Planetary Science Letters*, *289*(1–2), 87–104. https://doi.org/10.1016/j.epsl.2009.10.032

Keay, S. (1998). *The geological evolution of the Cyclades, Greece : Constraints from SHRIMP U-Pb geochronology*. Australian National University. http://oatd.org/oatd/record?record=handle%5C%3A1885%5C%2F145651

Kotowski, A. J., Cisneros, M., Behr, W. M., Stockli, D. F., Soukis, K., Barnes, J. D., & Ortega-Arroyo, D. (2022). Subduction, underplating, and return flow recorded in the Cycladic Blueschist Unit exposed on Syros, Greece. *Tectonics*, *41*(6), 6. https://doi.org/10.1029/2020TC006528

Lamont, T. N., Roberts, N. M. W., Searle, M. P., Gardiner, N. J., Gopon, P., Hsieh, Y.-T., Holdship, P., & White, R. W. (2023a). Contemporaneous crust-derived I- and S-type granite magmatism and normal faulting on Tinos, Delos, and Naxos, Greece: Constraints on Aegean orogenic collapse. *GSA Bulletin*. https://doi.org/10.1130/B36489.1

Lamont, T. N., Smye, A. J., Roberts, N. M. W., Searle, M. P., Waters, D. J., & White, R. W. (2023b). Constraints on the thermal evolution of metamorphic core complexes from the timing of high-pressure metamorphism on Naxos, Greece. *GSA Bulletin*. https://doi.org/10.1130/B36332.1

Laurent, V., Beaudoin, A., Jolivet, L., Arbaret, L., Augier, R., Rabillard, A., & Menant, A. (2015). Interrelations between extensional shear zones and synkinematic intrusions: The example of ikaria island (NE cyclades, Greece). *Tectonophysics*, *651-652*, 152–171. https://doi.org/10.1016/j.tecto.2015.03.020

Lecomte, E., Jolivet, L., Lacombe, O., Denèle, Y., Labrousse, L., & Le Pourhiet, L. (2010). Geometry and kinematics of Mykonos detachment, Cyclades, Greece: Evidence for slip at shallow dip. *Tectonics*, *29*(5), 5. https://doi.org/10.1029/2009TC002564

Lee, J., & Lister, G. S. (1992). Late Miocene ductile extension and detachment faulting, Mykonos, Greece. *Geology*, *20* (2), 121–124. https://doi.org/10.1130/0091-7613(1992)020<0121:LMDEAD>2.3.CO;2

Le Pichon, X., & Angelier, J. (1981). The Aegean Sea. *Philosophical Transactions of the Royal Society of London. Series A, Mathematical and Physical Sciences*, *300*(1454), 357–372.

Lister, G. S., & Baldwin, S. L. (1993). Plutonism and the origin of metamorphic core complexes. *Geology*, *21*(7), 607–610. https://doi.org/10.1130/0091-7613(1993)021<0607:PATOOM>2.3.CO;2

Lister, G. S., Banga, G., & Feenstra, A. (1984). Metamorphic core complexes of cordilleran type in the Cyclades, Aegean Sea, Greece. *Geology*, *12*(4), 221–225. https://doi.org/10.1130/0091-7613(1984)12<221:MCCOCT>2.0.CO;2

Martha, S. O., Dörr, W., Gerdes, A., Petschick, R., Schastok, J., Xypolias, P., & Zulauf, G. (2016). New structural and U–Pb zircon data from Anafi crystalline basement (Cyclades, Greece): Constraints on the evolution of a Late Cretaceous magmatic arc in the internal Hellenides. *International Journal of Earth Sciences*, *105*(7), 2031–2060. https://doi.org/10.1007/s00531-016-1346-8

Mehl, C., Jolivet, L., & Lacombe, O. (2005). From ductile to brittle: Evolution and localization of deformation below a crustal detachment (Tinos, Cyclades, Greece). *Tectonics*, *24*(4), 1–23. https://doi.org/10.1029/2004TC001767

Mehl, C., Jolivet, L., Lacombe, O., Labrousse, L., & Rimmele, G. (2007). Structural evolution of Andros (Cyclades, Greece): A key to the behaviour of a (flat) detachment within an extending continental crust. *Geological Society, London, Special Publications*, *291*(1), 41–73. https://doi.org/10.1144/SP291.3

Menant, A., Jolivet, L., Augier, R., & Skarpelis, N. (2013). The North Cycladic Detachment System and associated mineralization, Mykonos, Greece: Insights on the evolution of the Aegean domain. *Tectonics*, *32*(3), 433–452. https://doi.org/10.1002/tect.20037

Papanikolaou, D. (2009). Timing of tectonic emplacement of the ophiolites and terrane paleogeography in the Hellenides. *Lithos*, *108*(1-4), 262–280. https://doi.org/10.1016/j.lithos.2008.08.003

Papanikolaou, D. (2013). Tectonostratigraphic models of the Alpine terranes and subduction history of the Hellenides. *Tectonophysics*, *595-596*, 1–24. https://doi.org/10.1016/j.tecto.2012.08.008

Pe-Piper, G., Piper, D. J. W., & Matarangas, D. (2002). Regional implications of geochemistry and style of emplacement of Miocene I-type diorite and granite, Delos, Cyclades, Greece. *Lithos*, *60*(1-2), 47–66. https://doi.org/10.1016/S0024-4937(01)00068-8

Platt, J. P., Behr, W. M., & Cooper, F. J. (2015). Metamorphic core complexes: Windows into the mechanics and rheology of the crust. *Journal of the Geological Society*, *172*(1), 9–27. https://doi.org/10.1144/jgs2014-036

Rabillard, A., Jolivet, L., Arbaret, L., Bessière, E., Laurent, V., Menant, A., Augier, R., & Beaudoin, A. (2018). Synextensional granitoids and detachment systems within cycladic metamorphic core complexes (Aegean Sea, Greece): Toward a regional tectonomagmatic model. *Tectonics*, *37*(8), 2328–2362. https://doi.org/10.1029/2017TC004697

Ring, U., Glodny, J., Will, T., & Thomson, S. (2010). The Hellenic Subduction system: High-pressure metamorphism, exhumation, normal faulting, and large-scale extension. *Annual Review of Earth and Planetary Sciences*, *38*(1), 45–76. https://doi.org/10.1146/annurev.earth.050708.170910

Ring, U., Glodny, J., Will, T. M., & Thomson, S. (2011). Normal faulting on Sifnos and the South Cycladic Detachment System, Aegean Sea, Greece. *Journal of the Geological Society*, *168*(3), 751–768. https://doi.org/10.1144/0016-76492010-064

Ring, U., & Layer, P. W. (2003). High-pressure metamorphism in the Aegean, eastern Mediterranean: Underplating and exhumation from the Late Cretaceous until the miocene to recent above the retreating Hellenic subduction zone. *Tectonics*, *22*(3), 3. https://doi.org/10.1029/2001TC001350

Rosenbaum, G., Avigad, D., & Sánchez-Gómez, M. (2002). Coaxial flattening at deep levels of orogenic belts: Evidence from blueschists and eclogites on Syros and Sifnos (cyclades, Greece). *Journal of Structural Geology*, *24*(9), 1451–1462. https://doi.org/10.1016/S0191-8141(01)00143-2

Sànchez-Goméz, M., Avigad, D., & Heimann, A. (2002). Geochronology of clasts in allochthonous Miocene sedimentary sequences on Mykonos and Paros islands: Implications for back-arc extension in the Aegean Sea. *Journal of the Geological Society*, *159* (1), 45–60. https://doi.org/10.1144/0016-764901031

Searle, M. P., & Lamont, T. N. (2020). Compressional metamorphic core complexes, low-angle normal faults and extensional fabrics in compressional tectonic settings. *Geological Magazine*, *157*(1), 101–118. https://doi.org/10.1017/S0016756819000207

Searle, M. P., & Lamont, T. N. (2022). Compressional origin of the Aegean Orogeny, Greece. *Geoscience Frontiers*, *13*(2), 101049. https://doi.org/10.1016/j.gsf.2020.07.008

Seward, D., Vanderhaeghe, O., Siebenaller, L., Thomson, S., Hibsch, C., Zingg, A., Holzner, P., Ring, U., & Duchêne, S. (2009). Cenozoic tectonic evolution of Naxos Island through a multi-faceted approach of fission-track analysis. *Geological Society, London, Special Publications*, *321*(1), 179–196. https://doi.org/10.1144/SP321.9

Skarpelis, N. (2002). Geodynamics and evolution of the Miocene mineralisation in the Cycladic-Pelagonian Belt, Hellenides. *Bulletin of the Geological Society ot Greece* (6).

Varti-Mataranga, M., & Piper, W. J. D. (2004). Quaternary calcarenite ("POROS") of Mykonos, Delos and Rhenia, Cyclades islands, Greece. *Bulletin of the Geological Society of Greece*, *38*, XXXVI.

Xypolias, P., Iliopoulos, I., Chatzaras, V., & Kokkalas, S. (2012). Subduction- and exhumation-related structures in the cycladic blueschists: Insights from south Evia island (Aegean region, Greece). *Tectonics*, *31*(2). https://doi.org/10.1029/2011TC002946